

ADVANCED FUNCTIONAL MATERIALS

Supporting Information

for *Adv. Funct. Mater.*, DOI: 10.1002/adfm.202112902

Antibacterial Films Based on MOF Composites that Release Iodine Passively or Upon Triggering by Near-Infrared Light

Xu Han, Gerard Boix, Mateusz Balcerzak, Oscar Hernando Moriones, Mary Cano-Sarabia, Pilar Cortés, Neus Bastús, Victor Puentes, Montserrat Llagostera, Inhar Imaz, and Daniel Maspoch**

Supporting Information

Antibacterial films based on MOF composites that release iodine passively or upon triggering by near-infrared light

Xu Han[†], Gerard Boix[†], Mateusz Balcerzak, Oscar Hernando Moriones, Mary Cano-Sarabia, Pilar Cortés, Neus Bastús, Victor Puentes, Montserrat Llagostera, Inhar Imaz, Daniel MasPOCH**

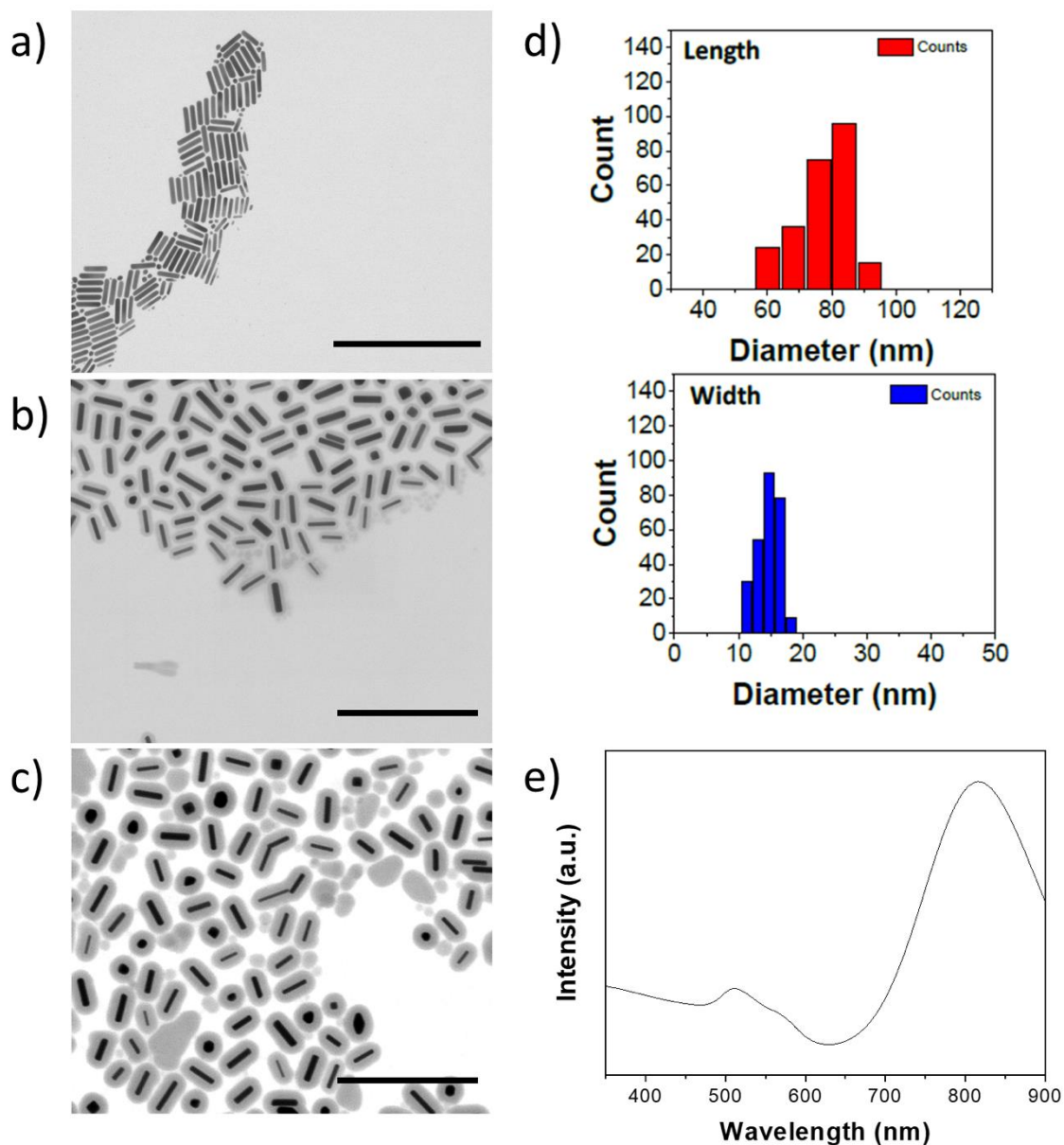


Figure S1. (a) Bright field STEM image of the synthesized AuNRs. (b) Bright field STEM image of the AuNR@SiO₂ after the first silica-shell coating. The shell size obtained after the coating was 17.5 ± 1.96 nm (c) Bright field STEM image of the AuNR@SiO₂ after the second silica-shell coating. The shell size obtained after the second coating was $30 \text{ nm} \pm 3 \text{ nm}$. (d) Length 77.5 ± 8.06 nm and width 14.6 ± 1.73 nm calculated size distribution of the synthesized AuNRs. The NPs presented an aspect ratio of: 5.00. (e) UV-Vis spectra of the synthesized AuNRs NPs, showing the LSRP peak maximum at 810 nm.

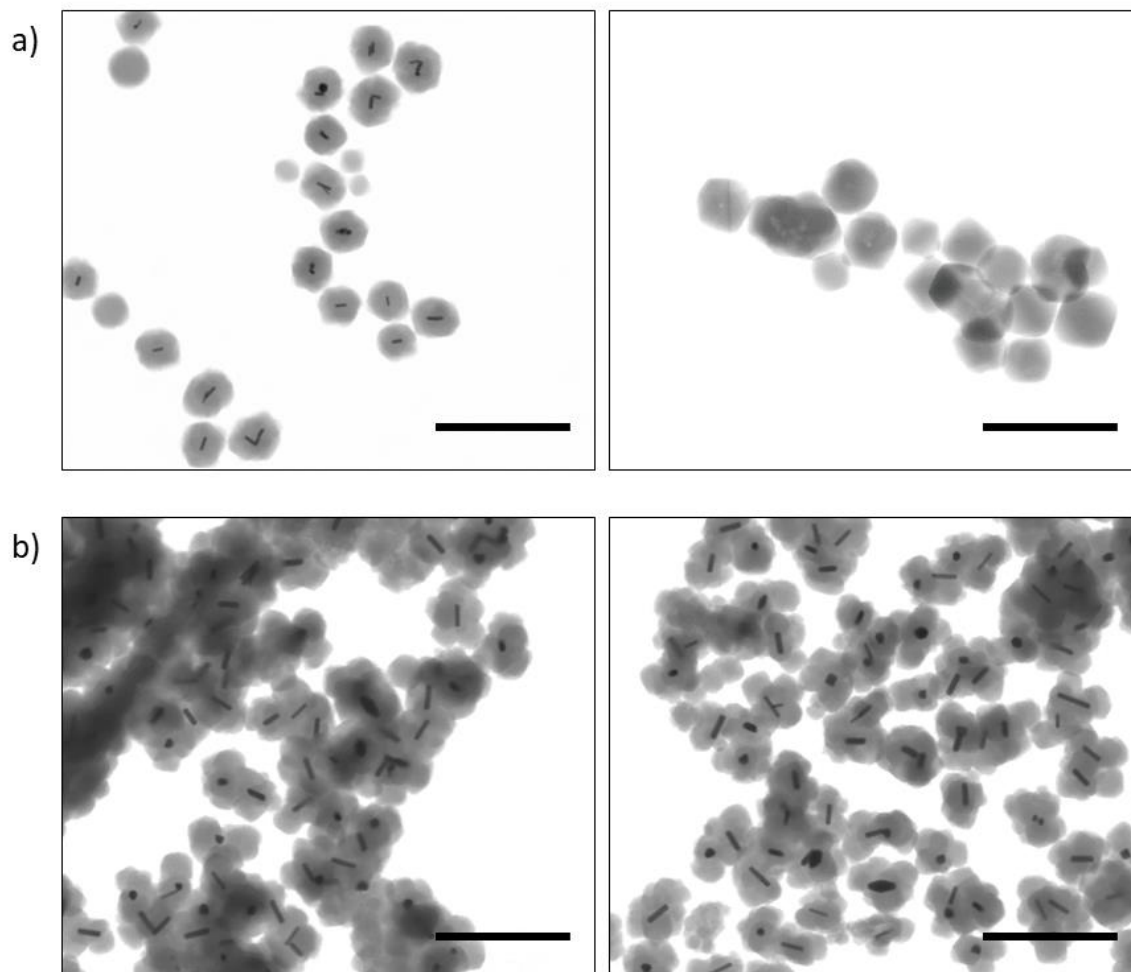


Figure S2. (a) STEM micrographs of synthesized AuNR@UiO-66 composite before (left) and after (right) exposure to iodine gas at 75 °C for 3 hours. Note that the AuNRs were etched after having been exposed to the iodine. (b) STEM micrographs of the AuNR@SiO₂@UiO-66 composite before (left) and after (right) exposure to iodine at 75 °C for 96 hours, confirming the stability of the silica-coated AuNRs. Scale bar: 500 nm.

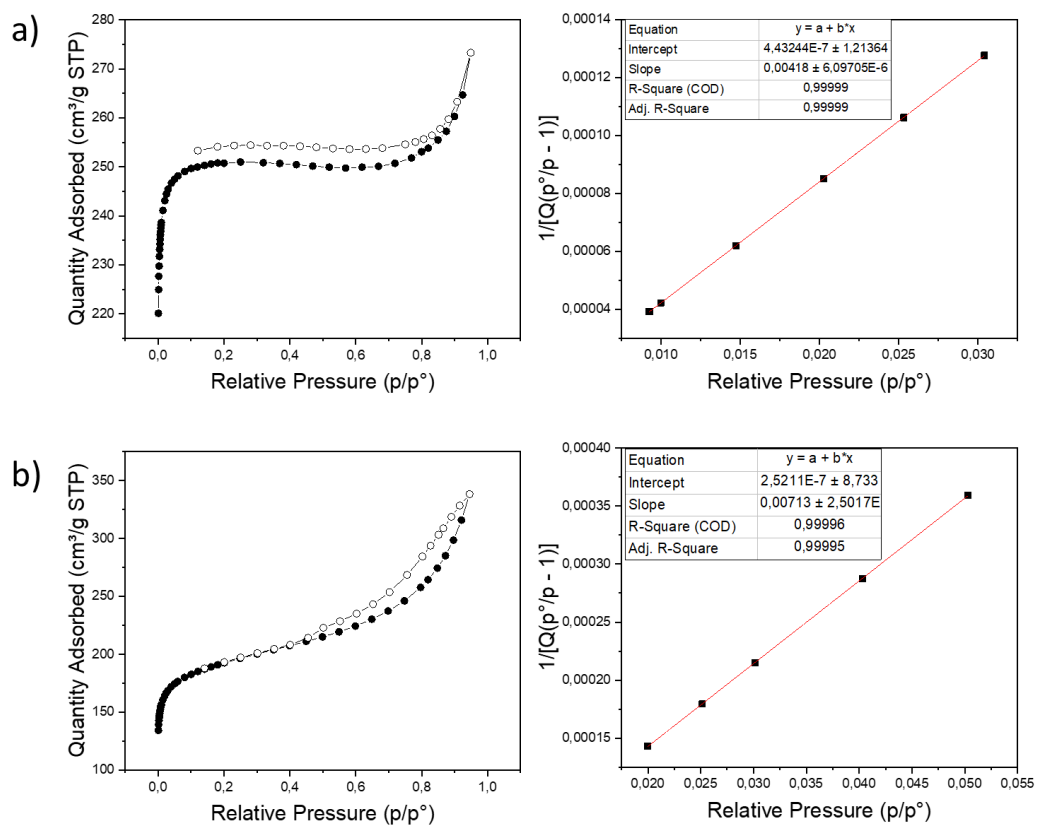


Figure S3. N₂-sorption isotherm measurements at 77 K, and corresponding BET plots, for UiO-66 microbeads (a) and AuNR@SiO₂@UiO-66 microbeads (b).

Material	Temperature (°C)		
	1000 mW cm ⁻²	224 mW cm ⁻²	52 mW cm ⁻²
UiO-66	25	24	24
AuNR@SiO ₂ @UiO-66	274	150	90
UiO-66 after desorption	48	32	26
AuNR@SiO ₂ @UiO-66 after desorption	269	145	86

Table S1. Summary of the maximum temperatures reached by each studied material upon irradiation with near-infrared lasers of different intensities.

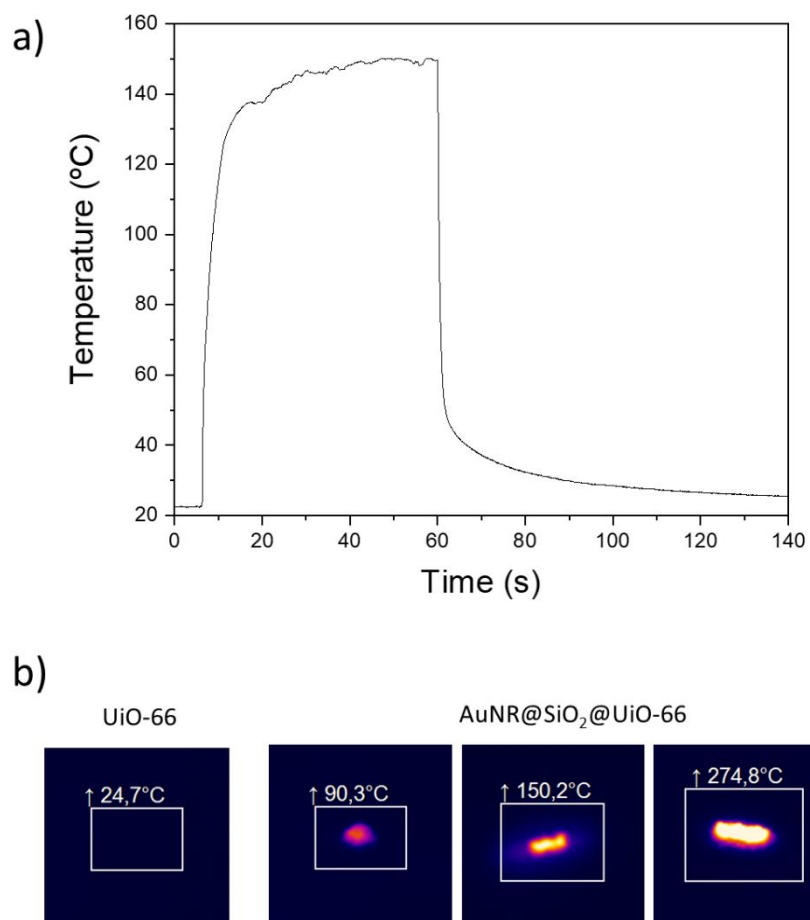


Figure S4. (a) Plot of time vs. temperature for AuNR@SiO₂@UiO-66 microbeads irradiated for 1 minute with near infrared light at an intensity of 224 mW cm⁻². (b) Thermal imaging of the UiO-66 (leftmost) when irradiated at 1000 mW cm⁻², and AuNR@SiO₂@UiO-66 microbeads when irradiated with an intensity of 52 mW cm⁻² (left), 224 mW cm⁻² (middle) and 1000 mW cm⁻² (right).

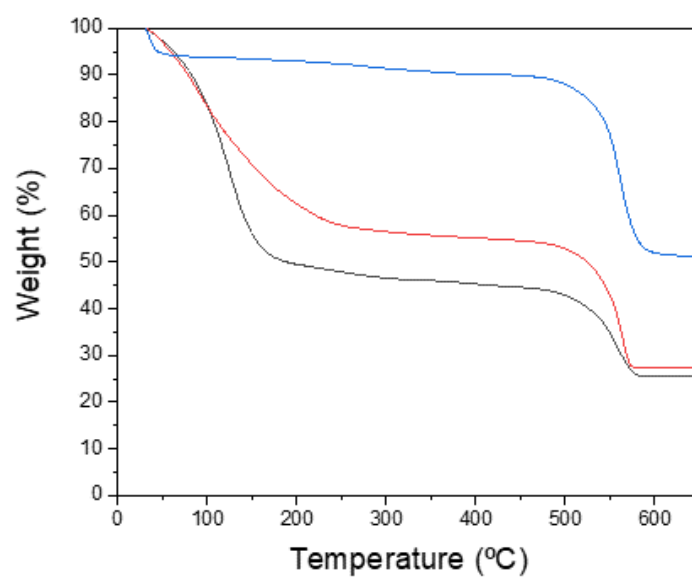


Figure S5. Thermogravimetric analysis curves for pristine UiO-66 microbeads (blue), iodine-loaded UiO-66 microbeads (black), and iodine-loaded AuNR@SiO₂@UiO-66 microbeads (red).

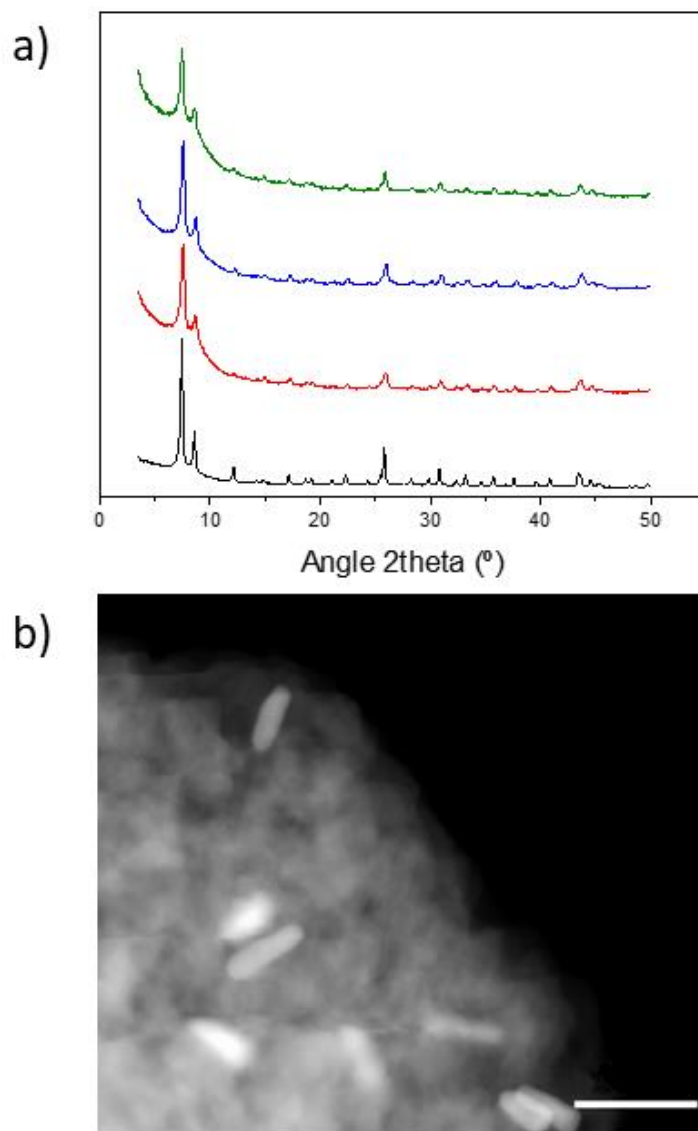


Figure S6. (a) PXRD spectra of pristine UiO-66 (black), pristine AuNR@SiO₂@UiO-66 (red), UiO-66 after desorption of iodine (blue), and AuNR@SiO₂@UiO-66 after desorption of iodine (green). (b) HAADF-STEM micrograph of AuNR@SiO₂@UiO-66 after 96-hour exposure to iodine at 75 °C. Scale bar: 100 nm.

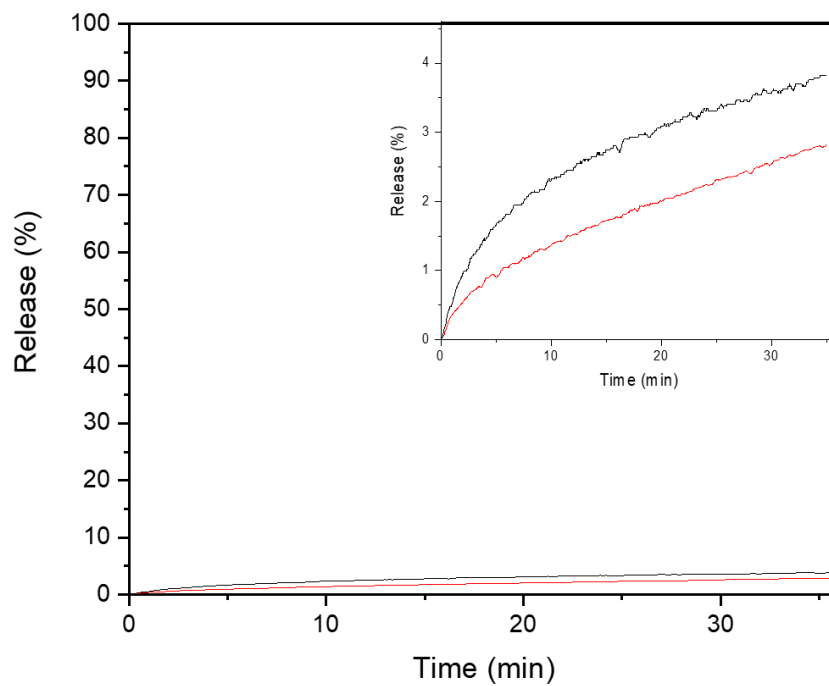


Figure S7. Release of iodine from $I_2@UiO-66$ microbeads (black) and $I_2@AuNR@SiO_2@UiO-66$ microbeads (red), without any laser irradiation. Inset: zoomed section of graph.

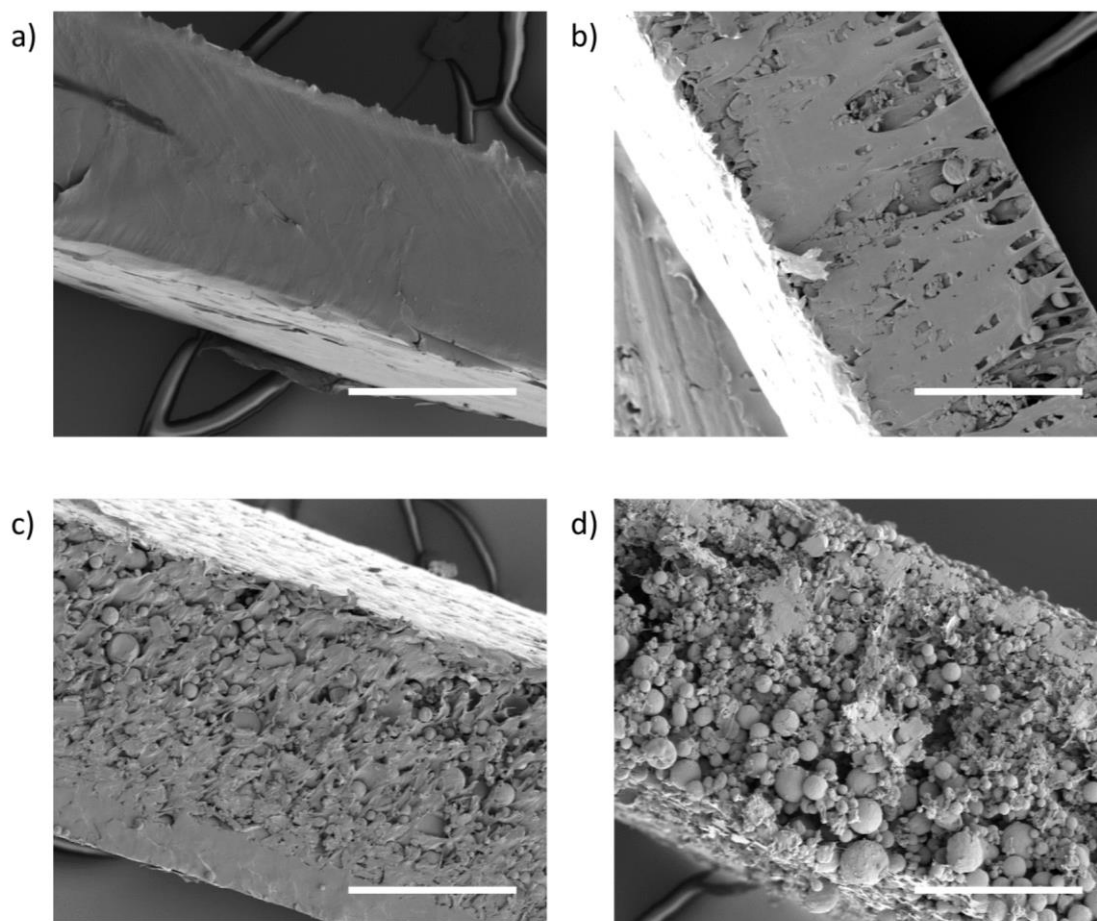


Figure S8. FE-SEM micrographs of cross-sections of the composite films containing AuNR@SiO₂@UiO-66 microbeads at 0% (a), 8% (b), 25% (c) and 46% (d) (w/w).

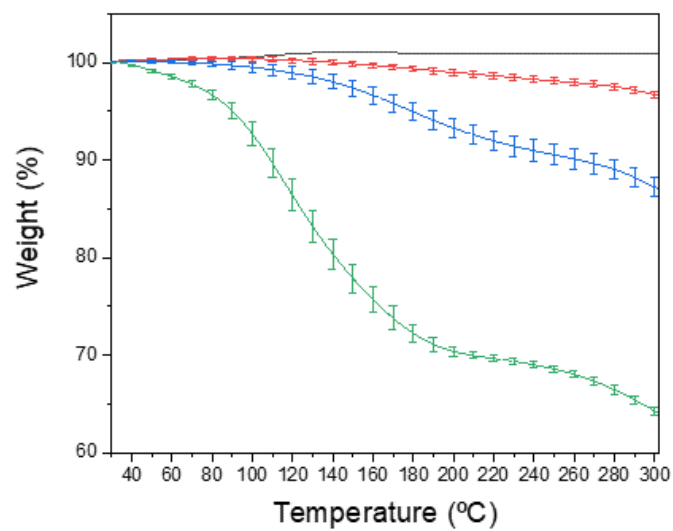


Figure S9. TGA curves of the iodine-loaded composite films containing AuNR@SiO₂@UiO-66 microbeads at 0% (black), 8% (red), 25% (blue) and 46% (green) (w/w).

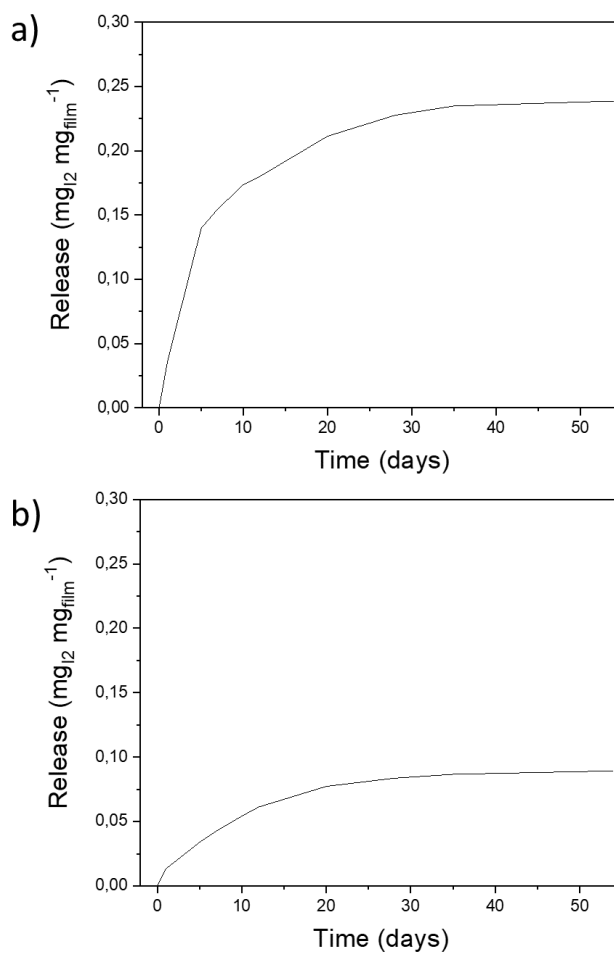


Figure S10. Iodine release over time from the composite films containing AuNR@SiO₂@UiO-66 microbeads at 46% (a) and 25% (b) (w/w), without any laser irradiation.

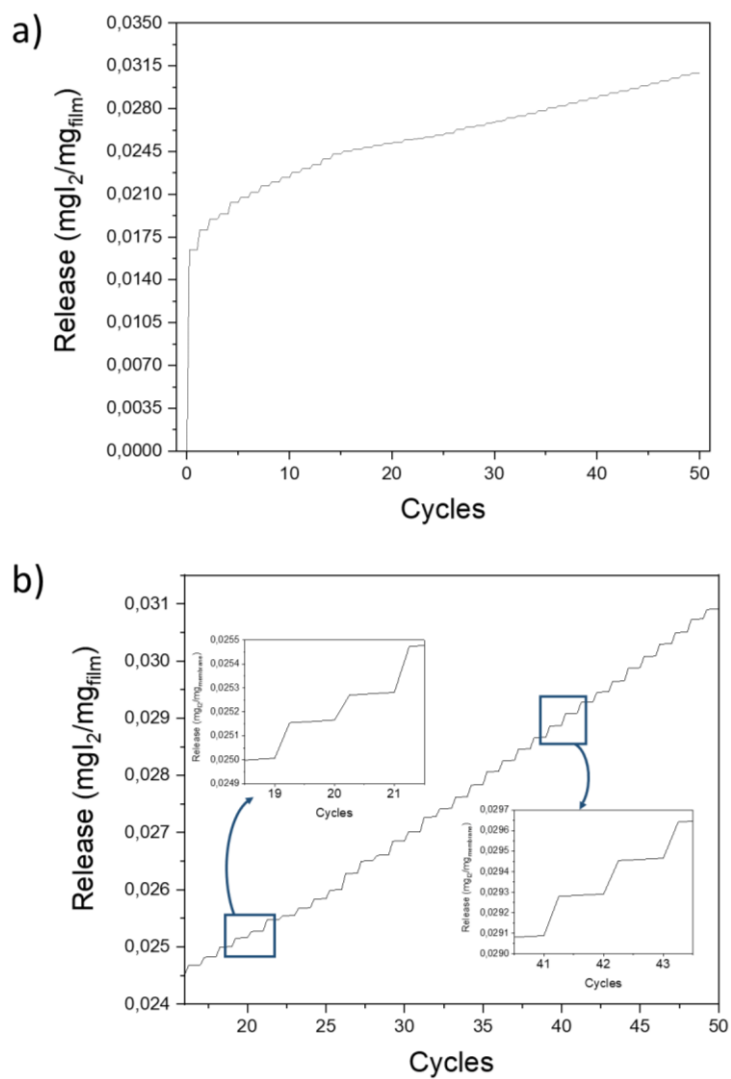


Figure S11 (a) Stepwise release of iodine from a composite film containing I₂@AuNR@SiO₂@UiO-66 microbeads at 25% (w/w) irradiated with NIR light at 224 mW cm⁻² and subjected to on/off switching. (b) Zoom on the stepwise release after its stabilization at the fifteenth cycle.

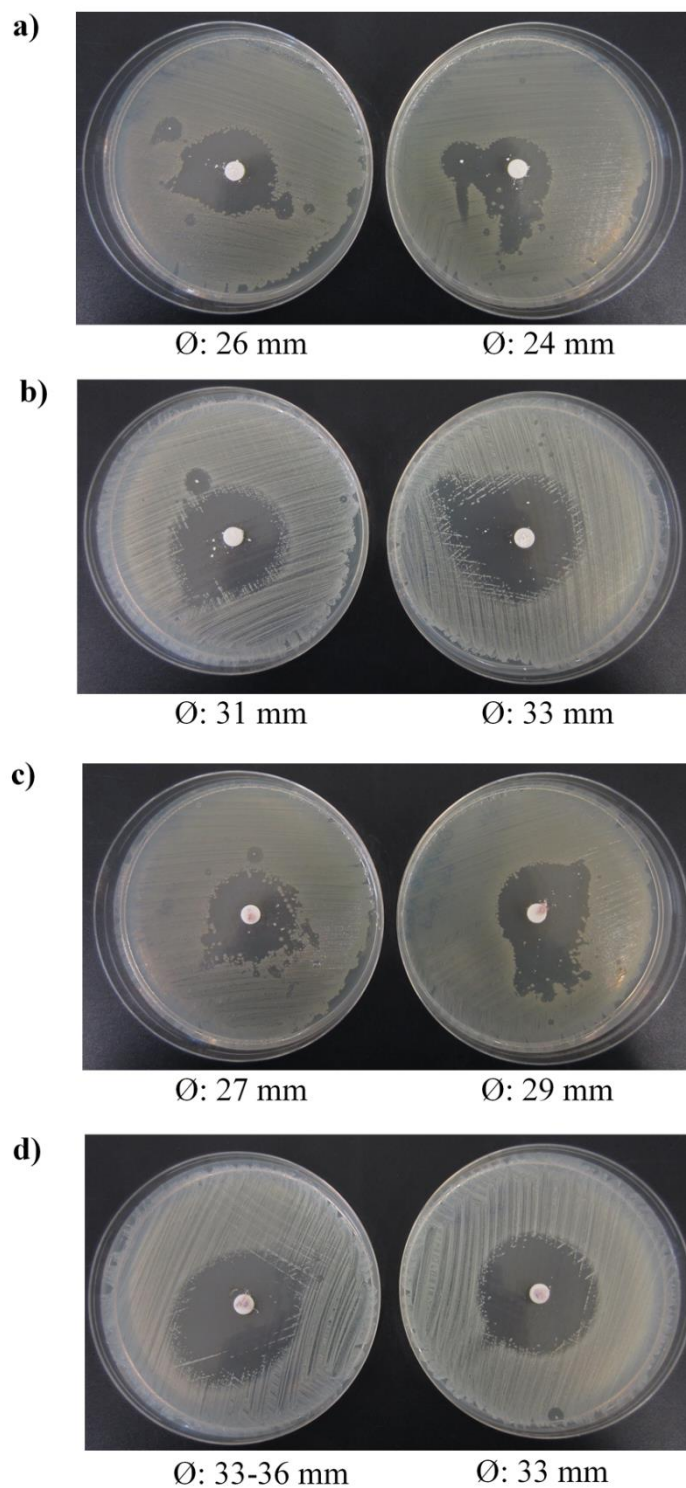


Figure S12. Growth-inhibition zones induced by $I_2@UiO-66$ microbeads (a, b) and $I_2@AuNR@SiO_2@UiO-66$ microbeads (c, d) against *E. coli* (a, c) or *S. aureus* (b, d) cultures, either after near-infrared light irradiation (left) or without irradiation (right). Ø: diameter of growth-inhibition zone. Disc diameter: 6 mm.

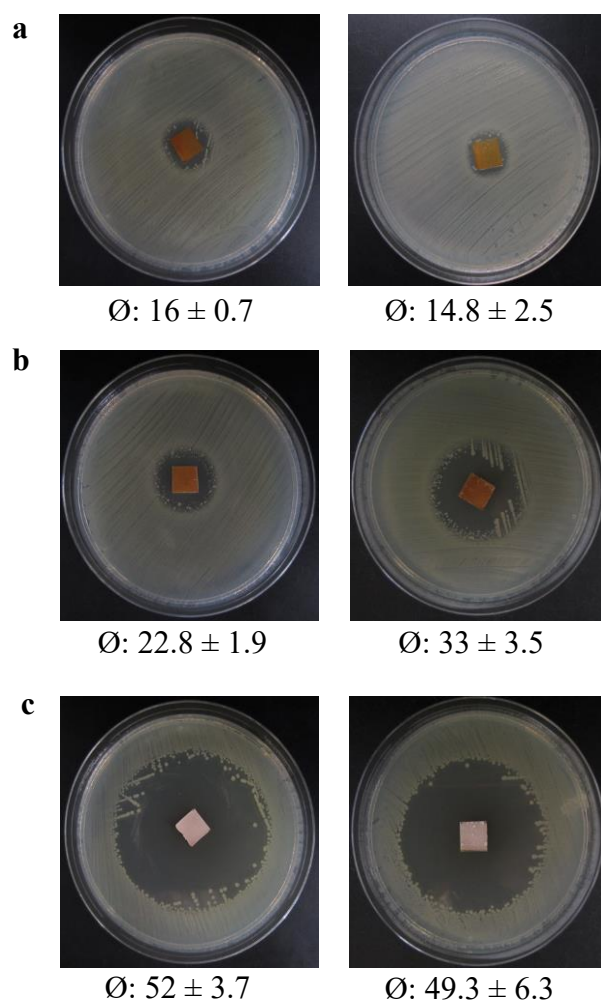


Figure S13. Growth-inhibition zones induced by square sections of composite films containing iodine-loaded AuNR@SiO₂@UiO-66 at 8% (a), 25% (b) and 46% (c) (w/w), against *E. coli* cultures, either after near-infrared light irradiation (left) or without irradiation (right). \varnothing : diameter of growth-inhibition zone. Film size: 1 cm². Values are the average of at least five replicates \pm standard deviation.

Table S2. Growth-inhibition of composite films prepared at different iodine-containing microbead-loadings (8%, 25% or 46%) and tested on *E. coli* cultures.

Composite (%)	\varnothing non irradiated with NIR (mm) ^a	\varnothing irradiated with NIR (mm) ^a
AuNR@SiO ₂ @UiO-66 (8%)	14.8 \pm 2.5	16 \pm 0.7
AuNR@SiO ₂ @UiO-66 (25%)	33 \pm 3.5 ^b	22.8 \pm 1.9
AuNR@SiO ₂ @UiO-66 (46%)	49.3 \pm 6.3 ^b	52 \pm 3.7 ^c

^a Each value is the average of at least five replicates \pm standard deviation.

^b Statistically significant differences between 25 and 46% compositions with respect to 8% within non irradiated group ($P < 0.0001$).

^c Statistically significant differences between 46% composition with respect to 8 and 25% within irradiated group ($P < 0.0001$).

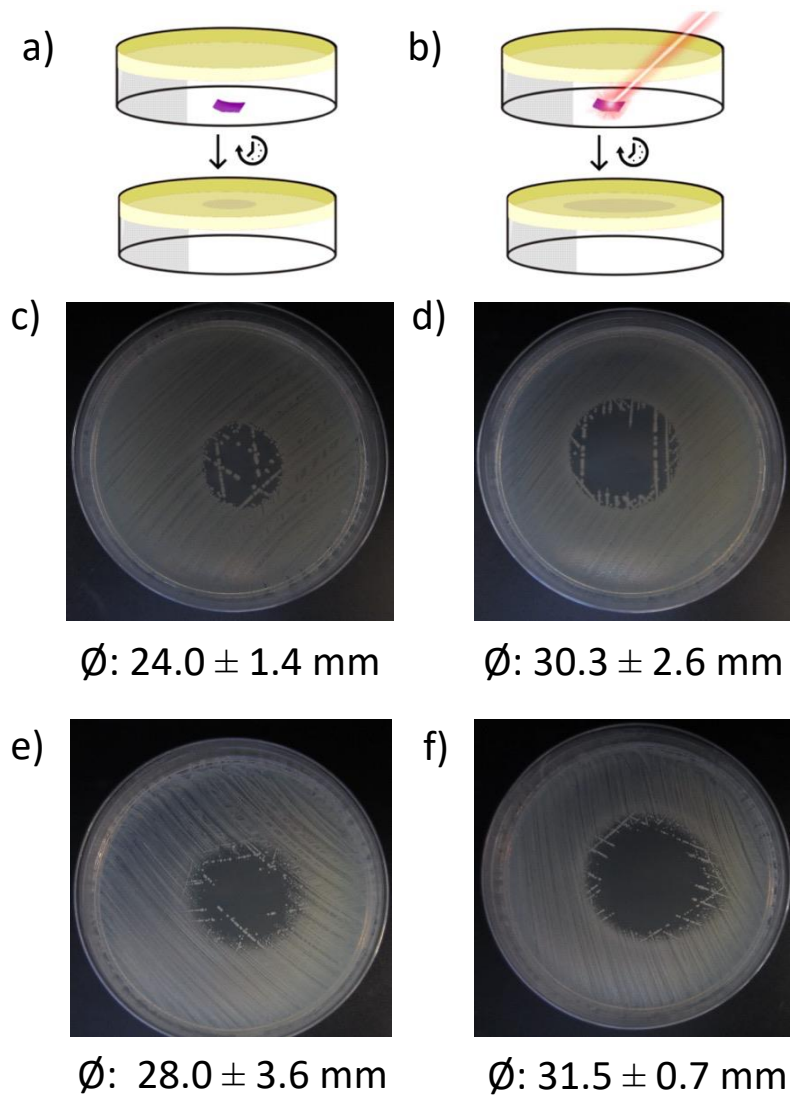


Figure S14. (a-b) Schematic illustrations of the two experiments performed to study the passive (a) or light-triggered (b) antibacterial performance of the films containing iodine-loaded UiO-66 microparticles. (c-f) Corresponding inhibition growth zones of *E. coli* (c-d) and *S. aureus* (e-f) cultures produced in composite films containing UiO-66 microparticles at 25% (w/w). Left and right: photographs taken after co-incubation of both film and agar plate inoculated with *E. coli* (c-d) and *S. aureus* (e,f) once the films had been removed. The films shown in (d,f) had been irradiated with NIR light. Ø: diameter of the growth-inhibition zone.

Table S3. Growth-inhibition diameters (\emptyset) in *E. coli* cultures created by composite films containing iodine-loaded AuNR@SiO₂@UiO-66 microbeads at 8% and 25%.

Composite (%)	\emptyset non irradiated with NIR (mm), film removed ^a	\emptyset irradiated with NIR (mm), film removed ^a	\emptyset non irradiated with NIR (mm), film not removed ^a
AuNR@SiO ₂ @UiO-66 (8%)	3.7 ± 4.3	15.6 ± 3.8 ^b	12.5 ± 2.4 ^c
AuNR@SiO ₂ @UiO-66 (25%)	27 ± 3.7	41.6 ± 2.7 ^b	38 ± 5 ^c

^a Each value is the average of at least four replicates ± standard deviation.

^b Statistically significant difference between non irradiated and irradiated with NIR film removed at 8% composite ($P = 0.0002$) and at 25% composite ($P < 0.0001$).

^c Statistically significant difference between non irradiated with NIR film removed and not removed at 8% composite ($P = 0.0047$) and at 25% composite ($P = 0.0023$).

Table S4. Growth-inhibition diameters (\emptyset) in *S. aureus* cultures created by composite films containing iodine-loaded AuNR@SiO₂@UiO-66 microbeads at 8% and 25%.

Composite (%)	\emptyset non irradiated with NIR (mm), film removed ^a	\emptyset irradiated with NIR (mm), film removed ^a	\emptyset non irradiated with NIR (mm), film not removed ^a
AuNR@SiO ₂ @UiO-66 (8%)	14.6 ± 5.7	19.5 ± 1.3	20.8 ± 3.4
AuNR@SiO ₂ @UiO-66 (25%)	25.3 ± 5.4	43.2 ± 4.3 ^b	45 ± 3.8 ^b

^a Each value is the average of at least four replicates ± standard deviation.

^b Statistically significant differences between irradiated with NIR film removed and non-irradiated film not removed regarding non irradiated film removed ($P < 0.0001$).